

# Blockade of PI3K $\gamma$ suppresses joint inflammation and damage in mouse models of rheumatoid arthritis

Montserrat Camps<sup>1,5</sup>, Thomas Rückle<sup>1,5</sup>, Hong Ji<sup>1,5</sup>, Vittoria Ardisson<sup>2</sup>, Felix Rintelen<sup>1</sup>, Jeffrey Shaw<sup>1</sup>, Chiara Ferrandi<sup>2</sup>, Christian Chabert<sup>1</sup>, Corine Gillieron<sup>1</sup>, Bernard Françon<sup>1</sup>, Thierry Martin<sup>1</sup>, Denise Gretener<sup>1</sup>, Dominique Perrin<sup>1</sup>, Didier Leroy<sup>1</sup>, Pierre-Alain Vitte<sup>1</sup>, Emilio Hirsch<sup>3</sup>, Matthias P Wymann<sup>4</sup>, Rocco Cirillo<sup>2</sup>, Matthias K Schwarz<sup>1</sup> & Christian Rommel<sup>1</sup>

Phosphoinositide 3-kinases (PI3K) have long been considered promising drug targets for the treatment of inflammatory and autoimmune disorders as well as cancer and cardiovascular diseases. But the lack of specificity, isoform selectivity and poor biopharmaceutical profile of PI3K inhibitors have so far hampered rigorous disease-relevant target validation. Here we describe the identification and development of specific, selective and orally active small-molecule inhibitors of PI3K $\gamma$  (encoded by *Pik3cg*). We show that *Pik3cg*<sup>-/-</sup> mice are largely protected in mouse models of rheumatoid arthritis; this protection correlates with defective neutrophil migration, further validating PI3K $\gamma$  as a therapeutic target. We also describe that oral treatment with a PI3K $\gamma$  inhibitor suppresses the progression of joint inflammation and damage in two distinct mouse models of rheumatoid arthritis, reproducing the protective effects shown by *Pik3cg*<sup>-/-</sup> mice. Our results identify selective PI3K $\gamma$  inhibitors as potential therapeutic molecules for the treatment of chronic inflammatory disorders such as rheumatoid arthritis.

Class I PI3Ks are dual-specific lipid and protein kinases involved in numerous intracellular signaling pathways. Class IA includes three catalytic subunits, p110 $\alpha$  (encoded by *Pik3ca*), p110 $\beta$  (encoded by *Pik3cb*) and p110 $\delta$  (encoded by *Pik3cd*), which form a complex with the SH2-containing regulatory p85 subunits, and are activated through tyrosine kinase signaling. Class IB p110 $\gamma$  is mainly activated by seven-transmembrane G-protein-coupled receptors (GPCRs), through its regulatory subunit p101 and G-protein  $\beta\gamma$  subunits<sup>1</sup>. Whereas expression of PI3K $\alpha$  and  $\beta$  is ubiquitous, that of PI3K $\gamma$  and  $\delta$  is mainly restricted to the hematopoietic system. *Pik3ca*<sup>-/-</sup> and *Pik3cb*<sup>-/-</sup> mice showed early-stage lethality during embryonic development<sup>2,3</sup>, whereas mice lacking expression or activity of PI3K $\gamma$  and  $\delta$  did not show any overt adverse phenotype. Mice lacking p110 $\delta$  function showed impaired B- and T-cell activation<sup>4-6</sup> as well as impaired mast cell activation<sup>7</sup>.

*Pik3cg*<sup>-/-</sup> mice showed a reduced chemoattractant-induced neutrophil respiratory burst, defective migration of macrophages and neutrophils to infection sites<sup>8-11</sup> and showed defects in adaptive immunity, including impaired T-cell activation and a reduced ability of dendritic cells to traffic to draining lymph nodes<sup>8,11</sup>. GPCR-mediated amplification of Fc $\epsilon$ RI-induced mast cell degranulation was also impaired in *Pik3cg*<sup>-/-</sup> mice, resulting in the absence of passive systemic anaphylaxis<sup>12</sup>.

Rheumatoid arthritis is a chronic systemic inflammatory disorder, affecting mainly joints, which affects about 1% of the population.

Despite extensive efforts, its etiology and pathogenesis remain poorly understood, and effective therapies with limited side effects are still lacking<sup>13</sup>. Collagen-induced arthritis (CIA), the most commonly used model for studying antirheumatic drugs, reproduces many of the pathogenic mechanisms detected in human rheumatoid arthritis, including increased cellular infiltration, synovial hyperplasia, pannus formation and erosion of cartilage and bone in the distal joints<sup>14</sup>. Participation of both T and B cells is required to initiate disease<sup>15</sup>, although direct administration of collagen II-specific antibodies ( $\alpha$ CII) reproduces arthritic features, independently of T and B cells<sup>16</sup>. In humans and in murine arthritis models, chemokines and other chemoattractants have been detected in inflamed joints and are responsible for recruitment of leukocytes, including macrophages and T cells, into the joints, which in most cases leads to the destructive processes, one of the hallmarks in the pathogenesis of rheumatoid arthritis<sup>15,17,18</sup>. A large body of evidence suggests the involvement of neutrophils and mast cells in both human rheumatoid arthritis and in mouse models of rheumatoid arthritis<sup>19-21</sup>. Neutrophils are not only the most abundant cell type in inflamed joints, they are also capable of inducing inflammatory response and damage<sup>22-25</sup>. Moreover, neutrophils seem to be important in both the initiation and perpetuation of experimental arthritis in mice<sup>26,27</sup>.

Several therapeutic strategies have been explored to prevent leukocyte chemotaxis and activation by blocking individual

<sup>1</sup>Serono Pharmaceutical Research Institute, Serono International S.A., 14, Chemin des Aulx, 1228 Plan-les-Ouates, Geneva, Switzerland. <sup>2</sup>LCG-RBM, Serono International S.A., Via Ribes 1, 10010 Collettero Giacosa, Italy. <sup>3</sup>Department of Genetics, Biology and Biochemistry, University of Torino, Via Santena 5bis, 10126 Torino, Italy. <sup>4</sup>Department of Clinical & Biological Sciences, Institute of Biochemistry & Genetics, Centre of Biomedicine, University of Basel, Mattenstrasse 28, 4058 Basel, Switzerland. <sup>5</sup>These authors contributed equally to this work. Correspondence should be addressed to C.R. (christian.rommel@serono.com).

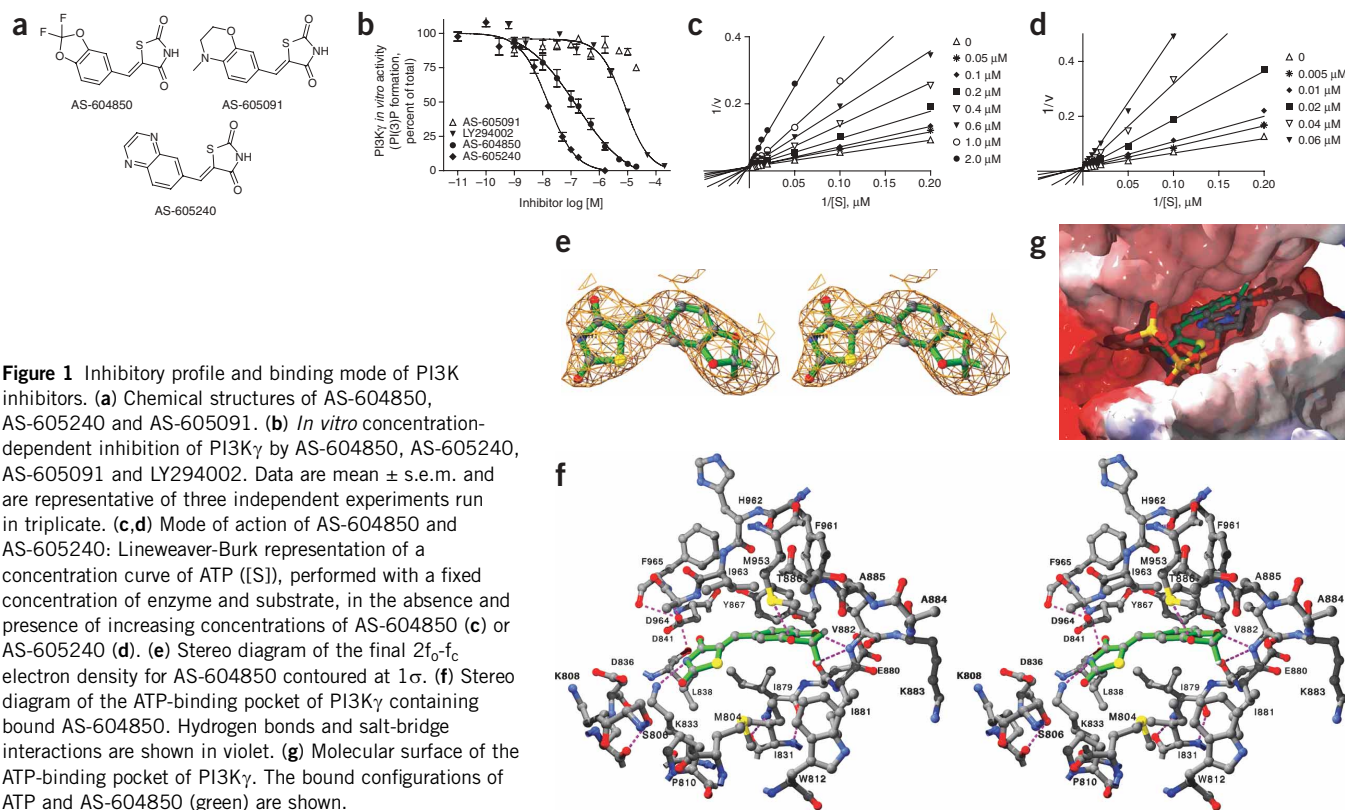


**Figure 1** Inhibitory profile and binding mode of PI3K inhibitors. **(a)** Chemical structures of AS-604850, AS-605240 and AS-605091. **(b)** *In vitro* concentration-dependent inhibition of PI3K $\gamma$  by AS-604850, AS-605240, AS-605091 and LY294002. Data are mean  $\pm$  s.e.m. and are representative of three independent experiments run in triplicate. **(c,d)** Mode of action of AS-604850 and AS-605240: Lineweaver-Burk representation of a concentration curve of ATP (1/S), performed with a fixed concentration of enzyme and substrate, in the absence and presence of increasing concentrations of AS-604850 (c) or AS-605240 (d). **(e)** Stereo diagram of the final  $2f_0-f_c$  electron density for AS-604850 contoured at  $1\sigma$ . **(f)** Stereo diagram of the ATP-binding pocket of PI3K $\gamma$  containing bound AS-604850. Hydrogen bonds and salt-bridge interactions are shown in violet. **(g)** Molecular surface of the ATP-binding pocket of PI3K $\gamma$ . The bound configurations of ATP and AS-604850 (green) are shown.

chemoattractants or their receptors<sup>17,28</sup>. Given that PI3K $\gamma$  has a pivotal role in mediating leukocyte chemotaxis and activation as well as mast cell degranulation, as shown by gene-targeting studies<sup>8,11,12</sup>, the pharmacological blockade of PI3K $\gamma$  might offer an innovative rationale-based therapeutic strategy for rheumatoid arthritis and other inflammatory diseases. Besides a strong medical hypothesis, the question of whether PI3K $\gamma$  is a valid and drug-responsive target for chronic inflammatory diseases has not been answered<sup>29</sup>.

We describe the discovery and development of a chemical series of potent and selective PI3K $\gamma$  inhibitors. Low-throughput enzyme screening and high-content cell-based screening, together with structure-based design, proved to be a crucial strategy for optimization of potency and selectivity of PI3K $\gamma$  small-molecule inhibitors. We report the biochemical and pharmacological characterization of two compounds, AS-604850 and AS-605240, which are shown to selectively inhibit PI3K $\gamma$  enzymatic activity as well as PI3K $\gamma$ -mediated signaling and chemotaxis *in vitro* and *in vivo*. We show that *Pik3cg*<sup>-/-</sup> mice are largely protected against  $\alpha$ CII-induced arthritis ( $\alpha$ CII-IA) and that this effect is associated with impaired neutrophil chemotaxis. Finally, we describe AS-605240 as an orally active small-molecule inhibitor of PI3K $\gamma$  that suppresses the progression of joint inflammation and damage in both lymphocyte-independent and lymphocyte-dependent mouse models of rheumatoid arthritis.

## RESULTS

### Structure-based discovery of PI3K $\gamma$ inhibitors

Screening with an automated *in vitro* lipid-kinase assay<sup>30</sup>, we have identified several small-molecule inhibitors of PI3K $\gamma$  that resulted ultimately in the design and synthesis of AS-604850 (5-(2,2-difluorobenzo[1,3]dioxol-5-ylmethylene)-thiazolidine-2,4-dione), AS-605240 (5-quinoxalin-6-ylmethylene-thiazolidine-2,4-dione) and AS-605091

(5-(4-methyl-3,4-dihydro-2H-benzo[1,4]oxazin-7-ylmethylene)-thiazolidine-2,4-dione), among others, from the same chemical series (Fig. 1a). To assess selectivity of the compounds for other isoforms of PI3K, we evaluated the enzymatic parameters, including  $K_m$  values for ATP, for each purified isoform (Supplementary Fig. 1 and Supplementary Table 1 online). Consequently, we made 50% inhibitory concentration ( $IC_{50}$ ) determinations for selectivity evaluation at ATP concentrations corresponding to experimental  $K_m$  values found for each isoform. AS-604850 and AS-605240 inhibit PI3K $\gamma$  *in vitro* with  $IC_{50}$  values of 0.250  $\mu$ M and 0.008  $\mu$ M, respectively, whereas AS-605091 has a substantially weaker effect ( $IC_{50} > 10 \mu$ M; Fig. 1b and Supplementary Table 2 online). To determine their mode of action, we performed inhibition experiments as a function of substrate concentration. Both AS-604850 and AS-605240 are ATP-competitive PI3K $\gamma$  inhibitors, with  $K_i$  values of 0.18  $\mu$ M and 0.0078  $\mu$ M, respectively (Fig. 1c,d). AS-604850 (Fig. 1e–g) and AS-605240 (data not shown) were soaked in crystals of human PI3K $\gamma$  and crystallographic data were collected at the Swiss Light Source.

Analysis of the crystallographic structures showed the binding of both molecules to the ATP-binding pocket of PI3K $\gamma$ , further validating their mechanism of action (Fig. 1f,g). Notably, the thiazolidinedione nitrogen forms a salt-bridge interaction with the side chain of Lys833, whereas the main-chain nitrogen of Val882 forms a hydrogen bond with either the oxygen of the 1,3-benzodioxole ring of AS-604850 or the nitrogen of the quinoxaline ring of AS-605240, respectively. A summary of crystallographic information is shown in Supplementary Table 3 online. In contrast to the well-known class I PI3K inhibitors wortmannin and LY294002, AS-604850 and AS-605240 are isoform-selective inhibitors of PI3K $\gamma$  with over 30-fold selectivity for PI3K $\delta$  and  $\beta$ , and 18- and 7.5-fold selectivity over PI3K $\alpha$ , respectively (Supplementary Table 2 online). In addition, both inhibitors at a

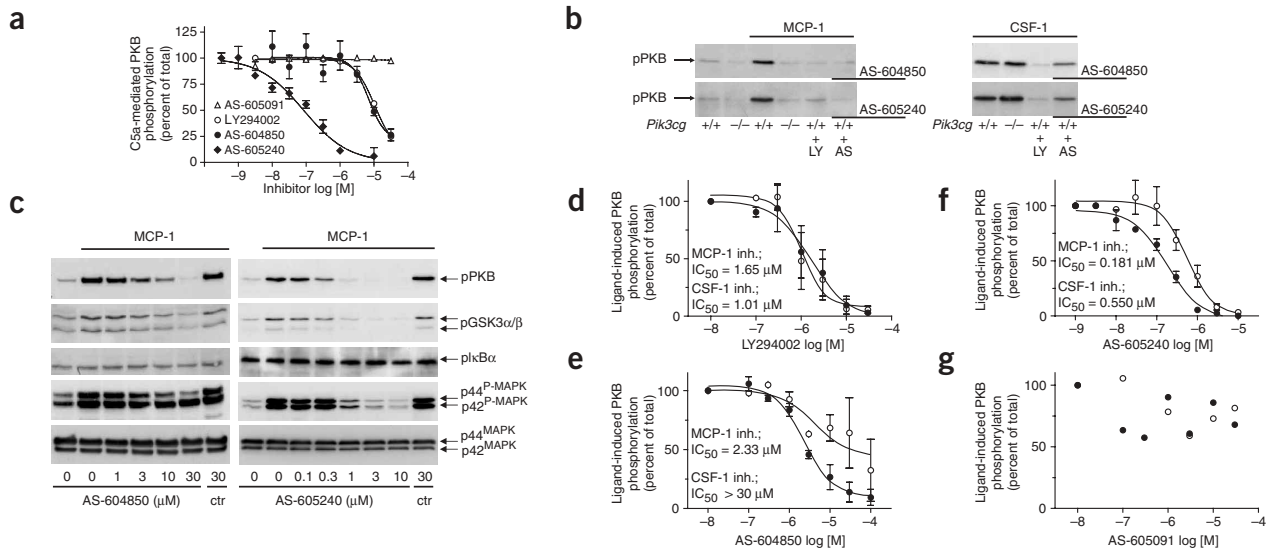


**Figure 2** PI3K $\gamma$  inhibitors block chemoattractant-mediated PKB phosphorylation in macrophages and primary monocytes. **(a)** Concentration-dependent inhibition of C5a-mediated PKB phosphorylation in RAW264 macrophages by AS-604850, AS-605240, AS-605091 and LY294002. Data ( $n = 6$ , mean  $\pm$  s.e.m.) are representative of at least two independent experiments. **(b)** Effect of AS-604850 (10  $\mu$ M), AS-605240 (1  $\mu$ M) and LY294002 (20  $\mu$ M) on MCP-1- and CSF-1-mediated PKB phosphorylation in primary monocytes from *Pik3cg*<sup>+/+</sup> or *Pik3cg*<sup>-/-</sup> mice. **(c)** Concentration-dependent inhibition of PI3K $\gamma$  downstream signaling by AS-604850, AS-605240 and AS-605091 in primary monocytes from *Pik3cg*<sup>+/+</sup> mice. **(d–g)** Concentration-dependent inhibition of PKB phosphorylation mediated by MCP-1 (closed circles) or CSF-1 (open circles) by PI3K $\gamma$  inhibitors in THP-1 monocytes.

concentration of 1  $\mu$ M did not have notable activity against a wide panel of protein kinases, at the corresponding  $K_m$  concentrations of ATP for each individual kinase (**Supplementary Fig. 2** online).

To further characterize the specificity of AS-604850 and AS-605240, the substantially less potent chemical derivative AS-605091 was used as a control in this study. All three compounds were tested at 10  $\mu$ M and did not show any notable effect on a large panel of receptors, unrelated enzymes and ion channels (data not shown). The *in vitro* physicochemistry properties and *in vivo* biopharmaceutical profile of AS-605240 are summarized in **Supplementary Fig. 3** online.

### Cell-signaling effects of small-molecule PI3K $\gamma$ inhibitors

Class IB PI3K $\gamma$ , in contrast to class IA, is directly activated by GPCRs, including the  $G_{\alpha i}$ -coupled chemokine receptors, leading to formation of phosphatidylinositol-(3,4,5)-triphosphate and consequent phosphorylation of PKB (also known as Akt) at the activity-regulatory residues Thr308 and Ser473. To assess whether AS-604850 and AS-605240 were capable of inhibiting PI3K $\gamma$  inside cells, we tested their ability to inhibit C5a-mediated PKB phosphorylation in RAW264 mouse macrophages. Whereas AS-605240 showed an IC<sub>50</sub> of 0.09  $\mu$ M, and AS-604850 of 10  $\mu$ M, similar to LY294002, the control compound AS-605091 did not show any effect up to 30  $\mu$ M (**Fig. 2a**). The higher cellular potency of AS-605240 compared to AS-604850 is explained not only by its higher *in vitro* potency but also its excellent cell permeability properties (data not shown).

GPCRs activate the PKB pathway primarily through class IB PI3K $\gamma$ , whereas single-transmembrane receptor tyrosine kinases utilize class IA PI3Ks. Thus, we next examined the capability of AS-604850 and AS-605240 to selectively inhibit chemokine-induced but not cytokine-induced PKB phosphorylation using bone marrow-derived monocytes (BMDMs). BMDMs isolated from *Pik3cg*<sup>+/+</sup> and *Pik3cg*<sup>-/-</sup> mice were stimulated either with the chemokine MCP-1 (also known as CCL2) binding to its corresponding GPCR, CCR2, or CSF-1, the ligand for the receptor tyrosine kinase c-Fms (**Fig. 2b**). MCP-1 strongly induced

phosphorylation of PKB in *Pik3cg*<sup>+/+</sup> monocytes, but not in *Pik3cg*<sup>-/-</sup> cells or *Pik3cg*<sup>+/+</sup> monocytes pretreated with LY294002 (**Fig. 2b**). In contrast to MCP-1, induction of PKB phosphorylation by CSF-1 was not affected in *Pik3cg*<sup>-/-</sup> monocytes (**Fig. 2b**), confirming that PI3K $\gamma$  is not primarily involved in the CSF-1–PI3K–PKB signaling cascade<sup>9,31</sup>. AS-604850 and AS-605240 blocked PKB phosphorylation induced by MCP-1 (**Fig. 2b**) and had little or no effect after stimulation with CSF-1 (**Fig. 2b**), indicating that both compounds mimic pharmacologically the loss of PKB phosphorylation in *Pik3cg*<sup>-/-</sup> monocytes. In contrast, the pan-PI3K inhibitor LY294002 blocked PKB phosphorylation equally after activation by either MCP-1 or CSF-1 (**Fig. 2b**). These results prove that receptor-mediated selective engagement of class IA versus class IB PI3K isoforms enables the validation of the selectivity of PI3K $\gamma$  inhibitors at the cellular level.

AS-604850 and AS-605240, but not the control compound AS-605091, inhibited MCP-1-mediated phosphorylation of PKB and its downstream substrates GSK3 $\alpha$  and  $\beta$  in a concentration-dependent manner (**Fig. 2c**). Notably, MCP-1-induced phosphorylation of p44/42 ERK (ERK1/2) MAPKs was also reduced, in a concentration-dependent manner, by AS-604850 and AS-605240, but not AS-605091 (**Fig. 2c**). This observation correlates with the partial loss of MCP-1-mediated ERK phosphorylation observed in *Pik3cg*<sup>-/-</sup> mice (data not shown) and is in agreement with previous findings<sup>32</sup>, thus indicating that ERK MAPKs signal downstream of PI3K $\gamma$  upon activation of CCR2 receptors. Neither AS-604850 nor the more potent AS-605240 altered at any concentration tested the phosphorylation status of I $\kappa$ B $\alpha$ , a phosphorylation-sensitive signal transducer unrelated to the PI3K $\gamma$  pathway (**Fig. 2c**).

Using the human monocytic cell line THP-1 to study the inhibition of PKB phosphorylation after activation by MCP-1 or CSF-1, we obtained similar results (**Fig. 2d–g**). AS-604850 and AS-605240 preferentially blocked MCP-1- rather than CSF-1-induced PKB phosphorylation, in a concentration-dependent manner. Whereas the IC<sub>50</sub> values for AS-605240 and AS-604850 on blocking MCP-1- or

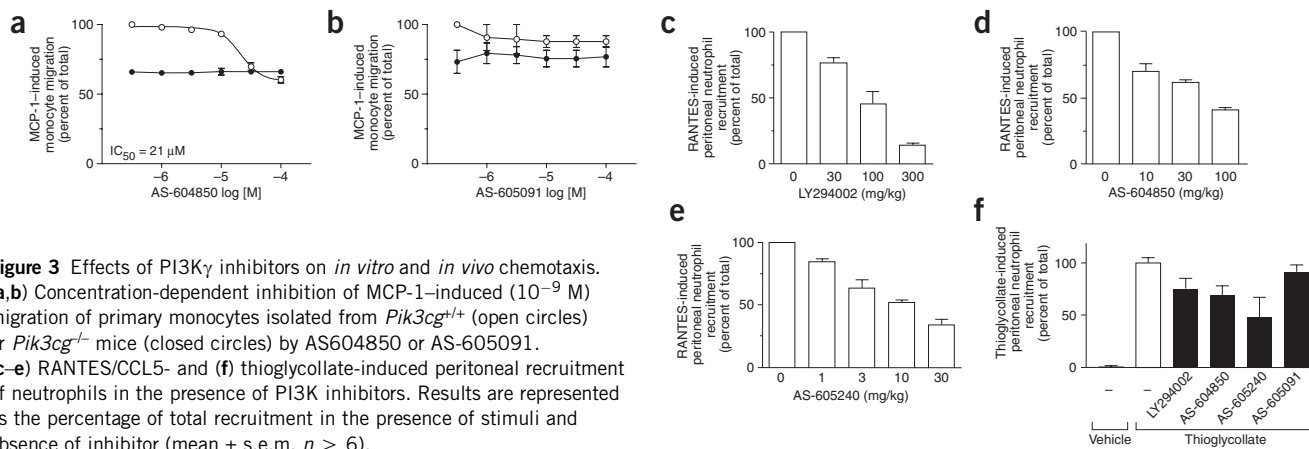


**Figure 3** Effects of PI3K $\gamma$  inhibitors on *in vitro* and *in vivo* chemotaxis. (a,b) Concentration-dependent inhibition of MCP-1-induced ( $10^{-9}$  M) migration of primary monocytes isolated from *Pik3cg*<sup>+/+</sup> (open circles) or *Pik3cg*<sup>-/-</sup> mice (closed circles) by AS604850 or AS-605091. (c–e) RANTES/CCL5- and (f) thioglycollate-induced peritoneal recruitment of neutrophils in the presence of PI3K inhibitors. Results are represented as the percentage of total recruitment in the presence of stimuli and absence of inhibitor (mean  $\pm$  s.e.m.  $n \geq 6$ ).

CSF-1-induced PKB phosphorylation showed a selectivity index of about three- to tenfold, respectively (Fig. 2e,f), LY294002, as expected, blocked MCP-1- and CSF-1-induced PKB phosphorylation with equal potencies (Fig. 2d). The control compound AS-605091 did not have any specific effect in this assay at concentrations up to 30  $\mu$ M (Fig. 2g). These data are consistent with the role of PI3K $\gamma$  isoform predominantly controlling phosphoinositide signaling downstream of GPCR of the G $\alpha_i$  class, such as chemokine receptors. With the exception of LY294002, none of the inhibitors tested showed any effect on cell viability (data not shown).

#### Cell-functional effects of small-molecule PI3K $\gamma$ inhibitors

Given that PI3K $\gamma$  regulates chemokine-induced migration of neutrophils, monocytes and macrophages<sup>8–10</sup>, we examined the effects of blocking PI3K $\gamma$  activity on MCP-1-induced chemotaxis in primary *Pik3cg*<sup>+/+</sup> and *Pik3cg*<sup>-/-</sup> mouse monocytes. MCP-1-induced migration is clearly, although not completely, abrogated in *Pik3cg*<sup>-/-</sup> compared to *Pik3cg*<sup>+/+</sup> monocytes. On the other hand, LY294002 did not further impair migration of the *Pik3cg*<sup>-/-</sup> monocytes (data not shown). These data confirm that the PI3K-dependent chemotactic response is almost exclusively controlled by the PI3K $\gamma$  isoform. AS-604850 blocked MCP-1-mediated chemotaxis in *Pik3cg*<sup>+/+</sup> monocytes in a concentration-dependent manner, with an IC<sub>50</sub> of 21  $\mu$ M, but did not affect chemotaxis in *Pik3cg*<sup>-/-</sup> cells (Fig. 3a), indicating that AS-604850 acts through PI3K $\gamma$ . The lack of inhibition in *Pik3cg*<sup>-/-</sup> monocytes suggests as well a lack of nonspecific effects of AS-604850. These results confirm the predicted inhibitory and specific effects of the compound on PI3K $\gamma$ . The control compound AS-605091 did not affect chemotaxis of primary monocytes in the presence or absence of PI3K $\gamma$  expression at any concentration tested (Fig. 3b).

#### PI3K $\gamma$ inhibitors reduce neutrophil chemotaxis *in vivo*

To evaluate the *in vivo* efficacy of PI3K $\gamma$  inhibitors in blocking leukocyte migration, we tested LY294002, AS-604850 and AS-605240 in two mouse models of peritonitis, either induced by RANTES (also known as CCL5) or thioglycollate, which induces release of multiple chemokines *in vivo*. As in many inflammatory processes, neutrophils are predominant in the initial influx of leukocytes, followed by monocytes-macrophages and lymphocytes<sup>33</sup>. Whereas the pan-PI3K inhibitor LY294002 reduced RANTES-induced peritoneal neutrophil recruitment, with a half-maximal efficacious dose (ED<sub>50</sub>) of 81.6 mg/kg (Fig. 3c), AS-604850 and AS-605240 showed higher efficacy with ED<sub>50</sub> values of 42.4 and 9.1 mg/kg, respectively (Fig. 3d,e). In the

thioglycollate-induced peritonitis model, oral administration of 10 mg/kg AS-604850 resulted in a 31% reduction of neutrophil recruitment (Fig. 3f). Notably, as in the CCL5 model, AS-605240 showed an ED<sub>50</sub> value of 10 mg/kg, in correlation with the percentage of reduction of neutrophil recruitment observed in *Pik3cg*<sup>-/-</sup> mice (data not shown). LY294002 was less efficacious, with an ED<sub>50</sub> value of 60 mg/kg (Fig. 3f). Treatment with the control compound AS-605091 did not show any notable effect (Fig. 3f). Taken together, these findings show that neutrophil chemotaxis can be inhibited *in vivo* by oral treatment with small-molecule inhibitors of PI3K $\gamma$ .

#### Inhibition of PI3K $\gamma$ ameliorates $\alpha$ CII-induced arthritis

To evaluate the consequences of interfering with PI3K $\gamma$  activity in joint inflammation, we used the passive  $\alpha$ CII-IA model<sup>16,34</sup>. After  $\alpha$ CII-IA induction, *Pik3cg*<sup>+/+</sup> mice developed severe paw swelling and joint inflammation with massive leukocyte infiltration, synovium proliferation, pannus formation and cartilage erosion, whereas *Pik3cg*<sup>-/-</sup> mice showed very mild paw swelling with a reduced number of infiltrating cells and less severe cartilage erosion (Fig. 4a,b). When evaluated with histopathological parameters, *Pik3cg*<sup>-/-</sup> mice had low scores in both synovial inflammation and cartilage erosion, compared to *Pik3cg*<sup>+/+</sup> mice (Fig. 4c). PI3K $\gamma$  deficiency thus protects against  $\alpha$ CII-IA symptoms.

Given that neutrophil infiltration has an essential role in  $\alpha$ CII-IA<sup>27</sup>, and that PI3K $\gamma$  is important for neutrophil migration, we analyzed neutrophil content in the arthritic joints and found fewer neutrophils in *Pik3cg*<sup>-/-</sup> mice compared to arthritic *Pik3cg*<sup>+/+</sup> controls (Fig. 4b,d).

To determine whether pharmacological inhibition of PI3K $\gamma$  is able to reduce  $\alpha$ CII-IA symptoms, we administered AS-605240 to *Pik3cg*<sup>+/+</sup> mice after arthritis onset (day 6; Fig. 4e). In this ‘therapeutic’ treatment protocol, mice received 50 mg/kg of AS-605240 orally, which resulted in a plasma concentration of approximately 3  $\mu$ M (Supplementary Fig. 3 online). AS-605240 substantially reduced clinical and histological signs of joint inflammation (Fig. 4e–g) to a similar extent to that of *Pik3cg*<sup>-/-</sup> mice (Fig. 4a–c). Toxicological examination showed that AS-605240 had no adverse secondary effects after the 5-d treatment period, with a cumulative dose of 500 mg/kg (data not shown). In summary, the PI3K $\gamma$  inhibitor AS-605240 mirrored PI3K $\gamma$  deficiency in protecting mice from development of  $\alpha$ CII-IA.

#### Oral administration of AS-605240 ameliorates CIA

To assess whether interference with PI3K $\gamma$  activity reduces joint inflammation when an adaptive immune response is suggested to be involved

in the pathogenesis of arthritis, as in human rheumatoid arthritis, we tested AS-605240 in a mouse model of collagen-induced arthritis.

Vehicle-treated mice developed disease clinically and histopathologically (Fig. 5a–c). Whereas indomethacin reduced synovial inflammation by 18% and cartilage erosion by 14%, AS-605240 after the same treatment period reduced these symptoms by 42% and 43%, respectively (Fig. 5b,c). Clinical symptoms, both digit inflammation (data not shown) and paw thickness, reverted when AS-605240 was administered using the therapeutic protocol, declining rapidly and staying mild for the remainder of the experimental period (Fig. 5a). AS-605240 treatment during the 7-d ‘therapeutic’ protocol also reduced synovium inflammation and cartilage erosion (Fig. 5b,c). We did not investigate bone erosion.

To determine the effect of AS-605240 treatment on neutrophil infiltration, we measured neutrophil accumulation in arthritic joints by histological analysis. Vehicle-treated CIA mice showed massive infiltration of neutrophils in addition to other leukocytes such as lymphocytes and macrophages, with an average of 48% neutrophil infiltrates in tissues surrounding the joints (Fig. 5b,d). In contrast, fewer infiltrates, in particular neutrophils, were found in CIA mice treated with AS-605240, both after semitherapeutic and therapeutic protocols, with an average of 29% and 24% neutrophil infiltrates, respectively (Fig. 5d).

In summary, we show that an orally active, selective PI3K $\gamma$  inhibitor suppresses joint inflammation and damage in a mouse model of rheumatoid arthritis.

## DISCUSSION

PI3K is a target of interest for modulation of inflammatory diseases<sup>29</sup>. Whereas the ubiquitous PI3K $\alpha$  and  $\beta$  isoforms regulate a variety of cell functions including survival and proliferation, the isoforms expressed mainly in the hematopoietic system, PI3K $\delta$  and  $\gamma$ , regulate immune responses<sup>35</sup>. Two classical PI3K inhibitors, wortmannin and LY294002, have been widely used to analyze and examine PI3K-mediated processes, but their inhibitory activity is not isoform specific<sup>36</sup>.

We have developed a potent, isoform-selective small-molecule PI3K $\gamma$  inhibitor, AS-604850. Crystallization of AS-604850 with PI3K $\gamma$  allowed the design of AS-605240, which showed substantially improved inhibitory potency toward PI3K $\gamma$ , while maintaining a favorable selectivity profile against the other PI3K isoforms as well as against a broad range of tyrosine and serine-threonine protein kinases. In addition, AS-605240 also shows high cellular permeability. In accordance with the concept of a PI3K $\gamma$  inhibitor being able to function as a ‘pan-chemokine receptor antagonist’ and thereby

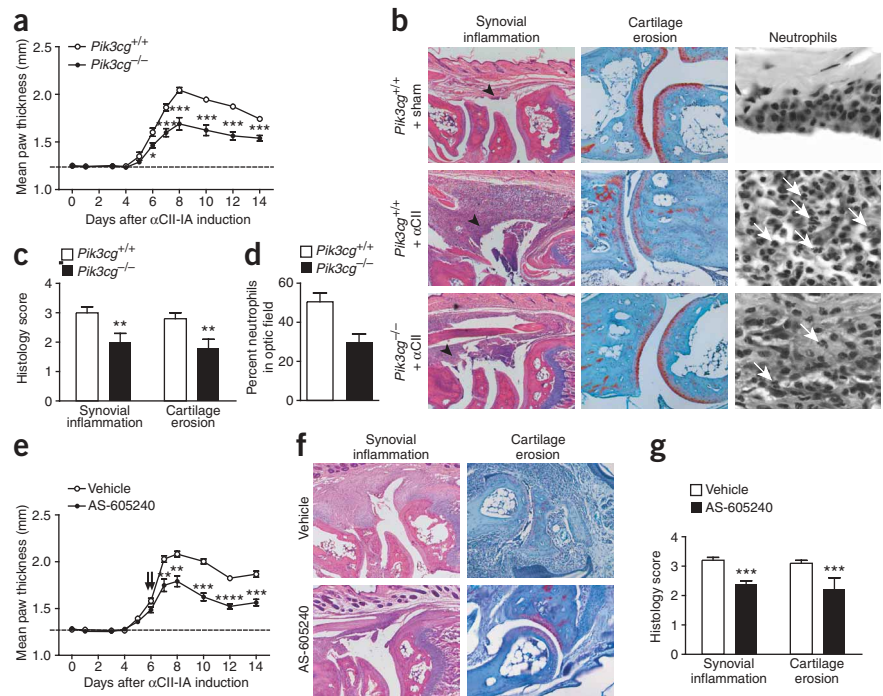


**Figure 4** Elimination of PI3K $\gamma$  function largely protects against  $\alpha$ CII-IA. (a) Mean paw thickness in *Pik3cg*<sup>-/-</sup> and *Pik3cg*<sup>+/+</sup> mice after  $\alpha$ CII-IA induction. Data ( $n \geq 5$ ) are representative of two independent experiments. (b) H&E (synovial inflammation, original magnification,  $\times 50$ ; neutrophils, original magnification,  $\times 1,000$ )– or safranin O (cartilage erosion, original magnification,  $\times 100$ )–stained representative joint sections from experiment shown in a, and sham-treated *Pik3cg*<sup>+/+</sup> mice. Arrowheads indicate areas shown at higher magnification in the neutrophil column. Arrows point to neutrophils. (c) Histological scores of inflammation and cartilage erosion from the experiment shown in a. (d) Neutrophil infiltration in joint sections from experiment shown in a. Data are expressed as percentage of neutrophils from total number of cells. (e)  $\alpha$ CII-IA development represented as mean paw thickness in *Pik3cg*<sup>+/+</sup> mice treated with vehicle or AS-605240 ( $n \geq 5$ ). Double arrow indicates initiation of the treatment. (f) H&E (original magnification,  $\times 50$ )– and safranin O (original magnification,  $\times 100$ )–stained representative joint sections from experiment shown in e. (g) Histological scores of synovial inflammation and cartilage erosion from the experiment shown in e. Data are mean  $\pm$  s.e.m. \* $P < 0.05$ , \*\* $P < 0.01$ , \*\*\* $P < 0.001$ . Dotted line indicates mean paw thickness level in healthy animals.

showing effects across different cell types and chemokine stimuli, both inhibitors were indeed found to inhibit PKB phosphorylation induced by C5a or MCP-1 in macrophages and monocytes, and consequently impaired chemotaxis *in vitro* and *in vivo*. Notably, as shown with *Pik3cg*<sup>-/-</sup> cells, the small-molecule PI3K $\gamma$  inhibitors showed little, if any, effect in inhibiting PKB phosphorylation in macrophages or primary monocytes upon stimulation with the non-GPCR ligand CSF-1. In contrast, LY294002 was unable to discriminate between MCP-1– and CSF-1–induced PKB phosphorylation, in agreement with its lack of selectivity amongst the different PI3K isoforms.

Because AS-605240 was found to be superior to AS-604850 across the whole panel of *in vitro* and *in vivo* assays, reflecting its higher inhibitory potency against the recombinant enzyme and its improved biopharmaceutical profile, this compound was therefore favored toward the progression into further long-term animal disease model studies. AS-605240 treatment mimicked the effect of PI3K $\gamma$  deficiency in mice, inhibiting *in vivo* neutrophil recruitment to joints. Interference with PI3K $\gamma$  expression (PI3K $\gamma$  deficiency) or activity (AS-605240 treatment) protected mice against development of  $\alpha$ CII-IA, a model that focuses on the effector phase of arthritis. These data support that inhibition of PI3K $\gamma$  mediates reduction of late-stage

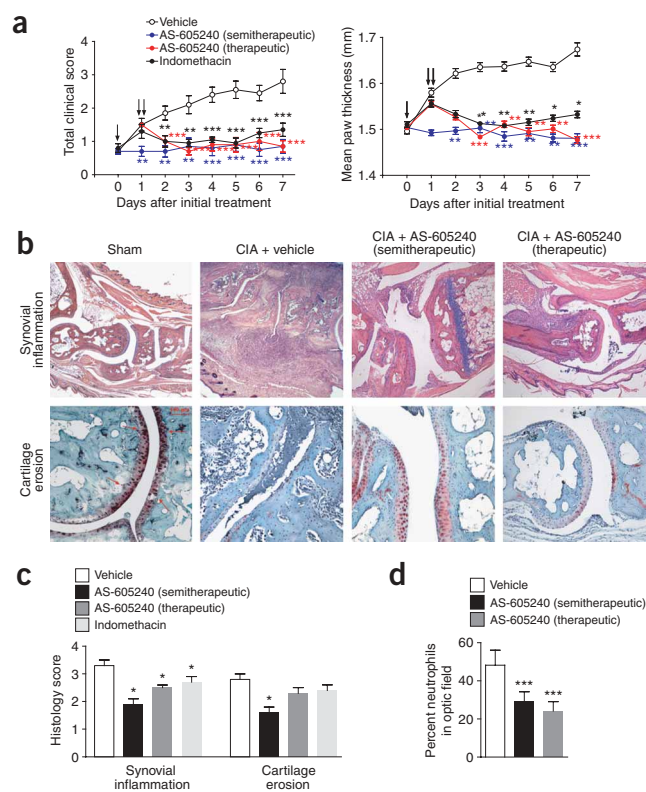


**Figure 5** Effects of AS-605240 in mouse CIA. **(a)** Total clinical scores and mean paw thickness ( $n = 10$ ) over 7 d from starting the 'semitherapeutic' (single arrow) or 'therapeutic' treatment (double arrow). **(b)** H&E (synovial inflammation, original magnification,  $\times 50$ ) or safranin O (cartilage erosion, original magnification,  $\times 100$ ) stained representative joint sections from experiment shown in **a**, and sham-treated wild-type mice. **(c)** Histological scores of inflammation and cartilage erosion from the experiment shown in **a**. **(d)** Neutrophil infiltration in joint sections from vehicle, AS-605240 semitherapeutic- and therapeutic-treated animals. Data represent the percentage of neutrophils from the total number of cells. Data are mean  $\pm$  s.e.m. \* $P < 0.05$ , \*\* $P < 0.01$ , \*\*\* $P < 0.001$ , compared with vehicle-treated group.

AS-605240 or vehicle after 7 d of therapeutic treatment. We observed a minor reduction of serum  $\alpha$ CII in mice treated with AS-605240 compared to animals treated with vehicle; however, this difference was not statistically significant (data not shown). Taking into account that AS-605240 ameliorated CIA clinical score as early as 1 d after administration in both semitherapeutic and therapeutic treatments, downregulation of the adaptive immune system through PI3K $\gamma$  inhibition does not seem to have a major role in the experimental setting used.

The efficacy of AS-605240 treatment in mouse rheumatoid arthritis models (AS-605240 also showed similar efficacy in a rat CIA model (data not shown)) supports PI3K $\gamma$  inhibition as a promising approach for the treatment of chronic inflammatory diseases. Moreover, in agreement with another published phenotype observed in *Pik3cg*<sup>-/-</sup> mice<sup>12</sup>, oral treatment with AS-605240 inhibited mast cell-dependent passive cutaneous anaphylaxis in rats (data not shown). The mechanisms of action examined suggest that PI3K $\gamma$  inhibition affects leukocyte recruitment and mast cell activation, and possibly other processes in the initiation and progression of chronic inflammation.

In conclusion, we have shown that pharmacological inhibition of PI3K $\gamma$  can effectively ameliorate chronic inflammatory disorders such as rheumatoid arthritis. As PI3K $\gamma$  is a shared downstream component of the majority of the promiscuous chemokine signaling pathways, it may represent an appropriate target for interfering with excessive leukocyte activation and migration in chronic inflammatory diseases.

## METHODS

**Recombinant human PI3K isoforms.** Expression and purification of recombinant human PI3K isoforms is described in **Supplementary Methods** online.

**In vitro PI3K $\gamma$  lipid kinase assay.** We performed PI3K $\gamma$  lipid kinase assay, based on neomycin-coated scintillation proximity assay bead technology (Amersham), in 96-well plates using [ $\gamma$ <sup>33</sup>P]ATP and phosphatidylinositol (Sigma) as substrates, as described<sup>30</sup>. For details, see **Supplementary Methods** online. Kinase assays for IC<sub>50</sub> determinations with PI3K $\alpha$ , PI3K $\beta$  and PI3K $\delta$  are described in **Supplementary Methods** online.

**Small-molecule PI3K $\gamma$  inhibitors.** Synthesis of AS-604850, AS-605240 and AS-605091 is as described<sup>40</sup>. Purification and crystallization<sup>41</sup> of PI3K $\gamma$  has been described previously<sup>42</sup>. Soaking of the inhibitors is described in **Supplementary Methods** online.

**C5a-mediated PKB phosphorylation in macrophages.** After 3 h starvation in serum-free medium, we pretreated RAW264 macrophages with inhibitors or DMSO for 30 min and stimulated them for 5 min with 50 nM of C5a (Sigma). We monitored PKB phosphorylation using phosphorylated Ser473 Akt-specific antibody (CST) and standard ELISA protocols.

**MCP-1- and CSF-1-mediated PKB phosphorylation in monocytes.** We pretreated THP-1 monocytes, which we had starved in serum-free medium for 3 h, with inhibitors or DMSO for 15 min and stimulated with 100 nM MCP-1 (R&D) for 30 s or 50  $\mu$ g/ml CSF-1 (Peprotec) for 5 min. We monitored PKB phosphorylation using phosphorylated Ser473 Akt-specific antibody. After

joint-specific inflammation. AS-605240 also inhibited arthritis progression in CIA, a model in which an adaptive immune response contributes to disease development similarly to the human disease<sup>14</sup>. AS-605240 was administered to mice using two treatment protocols: semitherapeutic (starting at disease onset) or therapeutic (begun once disease was established). AS-605240 treatment impaired arthritis progression when administered at disease onset and reverted it rapidly when given during established disease.

Deregulated cells that participate in adaptive and innate immune responses, such as T cell-mediated antigen-specific responses, T cell- and B cell-mediated autoantibody production, mast cell activation and local leukocyte infiltration, including neutrophils, are reported to have an essential role in the establishment of rheumatoid arthritis disease<sup>19,20,37</sup>. We show that after induction of arthritis in *Pik3cg*<sup>-/-</sup> mice, neutrophil infiltrates in joints are reduced compared to *Pik3cg*<sup>+/+</sup> mice. We also show that AS-605240 inhibited migration of neutrophils and monocytes and reduced neutrophil accumulation in the joints as well as disease development in both  $\alpha$ CII-IA and CIA models. Reduction of neutrophil infiltration is likely to be an important mechanism of action of PI3K $\gamma$  inhibition here, because disease in the  $\alpha$ CII-IA is largely lymphocyte independent and mainly neutrophil dependent<sup>16,27</sup>.

Nonetheless, as PI3K $\gamma$  inhibition is also efficient in CIA, in which T- and B-cell activation and subsequent  $\alpha$ CII production intervene in disease<sup>14,15,34</sup> it is possible that AS-605240 might have affected the adaptive immune components as well<sup>8</sup>. Moreover, another phenotype observed in *Pik3cg*<sup>-/-</sup> mice, namely impaired dendritic-cell migration to draining lymph nodes, resulting in defective T-cell activation<sup>11</sup>, may have also contributed to the protective effects of PI3K $\gamma$  inhibition in CIA, although this is a process predominantly involved in the induction phase<sup>38</sup>. We therefore measured serum  $\alpha$ CII titers, the end products of the adaptive immune response in the CIA model, which correlates with arthritis development<sup>39</sup>, in mice treated with

stripping and reprobing with PKB -specific antibodies, we scanned the blots and quantified them with a densitometer (Molecular Imageur FX; BioRad). We calculated PKB phosphorylation as the ratio between phosphorylated and total PKB for each lane and expressed it as the percentage of C5a-mediated phosphorylation in the absence of inhibitor.

**Preparation of mouse BMDMs and *in vitro* chemotaxis.** We isolated bone marrow cells as described<sup>31</sup>. After starving the cells in serum-free medium for 3 h and stimulating them with either MCP-1 or CSF-1, we performed western blotting as described<sup>31</sup>. For *in vitro* chemotaxis, we applied 10<sup>7</sup> BMDMs/ml, in medium containing 0.5% BSA and inhibitors or DMSO to the upper chamber (transwell 5 µm pore size, COSTAR) and we added 600 µl of medium containing MCP-1 and inhibitors or DMSO to the lower chamber. After 3 h incubation, we quantified cells from the lower chamber with a Beckman Coulter AcT 5diffTM.

**Oral treatment with PI3K inhibitors.** We dissolved PI3K inhibitors in vehicle (0.5% carboxymethylcellulose/0.25% Tween-20 (Sigma)) and adjusted the solution to 10 ml/kg of body weight.

**Mice.** We purchased Balb/c, C3H and DBA/1 mice from Charles River Laboratories. PI3Kγ-deficient (*Pik3cg*<sup>-/-</sup>) mice have been previously described<sup>9</sup>. *Pik3cg*<sup>-/-</sup> mice were backcrossed with C57Bl/6 for seven generations, with intercross to produce mutant *Pik3cg*<sup>-/-</sup> and control (*Pik3cg*<sup>+/+</sup>) littermates as experimental animals. We used 6–12-week-old mice in all experiments. All protocols using and maintaining animals were approved by the Swiss Veterinary Authority (Office Vétérinaire Cantonal) in Geneva or according to the European Council Directive 86/609/EEC and the Italian Ministry guidelines (decree 116/92), respectively.

**RANTES- and thioglycollate-induced peritonitis.** We intraperitoneally injected female Balb/C or C3H mice with human recombinant RANTES (0.5 mg/kg in 200 µl saline) or thioglycollate (40 ml/kg) (Sigma), respectively. Thirty or fifteen minutes before injection of human recombinant RANTES or thioglycollate, we orally administered PI3K inhibitors or vehicle. Four hours after injection, mice were killed and cells from the peritoneal cavity were isolated and characterized in a Beckman Coulter AcT 5diffTM.

**αCII-IA.** We injected mice intravenously with 4 mg Arthrogen-CIA type II collagen-specific monoclonal antibodies (αCII) (Chemicon) at day 0 and day 1 and 50 µg of lipopolysaccharide intraperitoneally at day 3. We measured paw thickness with a 0.01 mm precision caliper (Blet). We calculated mean paw thickness from the four paws of each individual mouse.

**Collagen-induced arthritis (CIA).** We injected male DBA/1 mice intradermally with 0.2 mg of bovine type II collagen (Chondrex) in complete Freund adjuvant (DIFCO). We measured paw thickness with a 0.01 mm precision caliper (MOD). We calculated mean paw thickness as described above. Clinical score evaluation is detailed in **Supplementary Methods** online. We treated each individual mouse assigned to the semitherapeutic or therapeutic treatment only when its total clinical score achieved 0.5 or 1.5, respectively. We treated mice orally with 50 mg/kg AS-605240 twice a day for 7 d. Indomethacin (2 mg/kg, administered orally in water, semitherapeutic treatment), was used as reference.

**Histological evaluation and statistical analysis.** See **Supplementary Methods** online.

**Accession codes.** Protein Data Bank accession codes: PI3Kγ-AS-604850, 2A4Z. PI3Kγ-AS-605240, 2A5U. GenBank accession codes: *PIK3CG*, accession number AF327656. *PIK3CA*, accession number U79143. *PIK3CB*, accession number S67334. *PIK3CD*, accession number, U86453. *PIK3R1*, accession number M61906.

*Note: Supplementary information is available on the Nature Medicine website.*

#### ACKNOWLEDGMENTS

We thank E. Ammanati, M. Carbonatto and S. Carboni for technical support and P. Gaillard, D. Church, T. Vallotton-Grippi, M. Maio and D. Covini for support in chemistry, A. Proudfoot's team for protein chemistry and C. Retzler and J. Hassa for advice. We are thankful to R. Williams for advice and technical support for crystallization. We further thank B. Vanhaesebroeck, K. Okkenhaug, R. Wetzker and in particular A. Carrera for support, advice and enthusiasm throughout the project, L. Stephens for advice and K. Jeffrey for critical reading of the manuscript.

We are grateful to C. Hebert for graphic support, C. Mark for editorial support and P. Cavioli for administrative assistance. We especially thank M. Kosco-Vilbois for encouragement when this project was initiated. We thank S. Arkininstall and T. Wells for support throughout the entire study. This work was supported by European Union Fifth Framework Program QLGI-2001-02171 to E.H., M.P.W. and C.R.

#### COMPETING INTERESTS STATEMENT

The authors declare that they have no competing financial interests.

Received 3 May; accepted 7 July 2005

Published online at <http://www.nature.com/naturemedicine/>

- Vanhaesebroeck, B. *et al.* Synthesis and function of 3-phosphorylated inositol lipids. *Annu. Rev. Biochem.* **70**, 535–602 (2001).
- Bi, L., Okabe, I., Bernard, D.J., Wynshaw-Boris, A. & Nussbaum, R.L. Proliferative defect and embryonic lethality in mice homozygous for a deletion in the p110alpha subunit of phosphoinositide 3-kinase. *J. Biol. Chem.* **274**, 10963–10968 (1999).
- Bi, L., Okabe, I., Bernard, D.J. & Nussbaum, R.L. Early embryonic lethality in mice deficient in the p110beta catalytic subunit of PI 3-kinase. *Mamm. Genome* **13**, 169–172 (2002).
- Okkenhaug, K. *et al.* Impaired B and T cell antigen receptor signaling in p110delta PI 3-kinase mutant mice. *Science* **297**, 1031–1034 (2002).
- Clayton, E. *et al.* A crucial role for the p110delta subunit of phosphatidylinositol 3-kinase in B cell development and activation. *J. Exp. Med.* **196**, 753–763 (2002).
- Jou, S.T. *et al.* Essential, nonredundant role for the phosphoinositide 3-kinase p110delta in signaling by the B-cell receptor complex. *Mol. Cell. Biol.* **22**, 8580–8591 (2002).
- Ali, K. *et al.* Essential role for the p110delta phosphoinositide 3-kinase in the allergic response. *Nature* **431**, 1007–1011 (2004).
- Sasaki, T. *et al.* Function of PI3Kgamma in thymocyte development, T cell activation, and neutrophil migration. *Science* **287**, 1040–1046 (2000).
- Hirsch, E. *et al.* Central role for G protein-coupled phosphoinositide 3-kinase gamma in inflammation. *Science* **287**, 1049–1053 (2000).
- Li, Z. *et al.* Roles of PLC-beta2 and -beta3 and PI3Kgamma in chemoattractant-mediated signal transduction. *Science* **287**, 1046–1049 (2000).
- Del Prete, A. *et al.* Defective dendritic cell migration and activation of adaptive immunity in PI3Kgamma-deficient mice. *EMBO J.* **23**, 3505–3515 (2004).
- Laffargue, M. *et al.* Phosphoinositide 3-kinase gamma is an essential amplifier of mast cell function. *Immunity* **16**, 441–451 (2002).
- Smolen, J.S. & Steiner, G. Therapeutic strategies for rheumatoid arthritis. *Nat. Rev. Drug Discov.* **2**, 473–488 (2003).
- Trentham, D.E. Collagen arthritis as a relevant model for rheumatoid arthritis. *Arthritis Rheum.* **25**, 911–916 (1982).
- Stuart, J.M., Townes, A.S. & Kang, A.H. Collagen autoimmune arthritis. *Annu. Rev. Immunol.* **2**, 199–218 (1984).
- Terato, K. *et al.* Induction of arthritis with monoclonal antibodies to collagen. *J. Immunol.* **148**, 2103–2108 (1992).
- Szekanecz, Z., Kim, J. & Koch, A.E. Chemokines and chemokine receptors in rheumatoid arthritis. *Semin. Immunol.* **15**, 15–21 (2003).
- Feldmann, M., Brennan, F.M. & Maini, R.N. Role of cytokines in rheumatoid arthritis. *Annu. Rev. Immunol.* **14**, 397–440 (1996).
- Edwards, S.W. & Hallett, M.B. Seeing the wood for the trees: the forgotten role of neutrophils in rheumatoid arthritis. *Immunol. Today* **18**, 320–324 (1997).
- Benoist, C. & Mathis, D. Mast cells in autoimmune disease. *Nature* **420**, 875–878 (2002).
- Lee, D.M. *et al.* Mast cells: a cellular link between autoantibodies and inflammatory arthritis. *Science* **297**, 1689–1692 (2002).
- Chatham, W.W. *et al.* Degradation of human articular cartilage by neutrophils in synovial fluid. *Arthritis Rheum.* **36**, 51–58 (1993).
- Kitsis, E. & Weissmann, G. The role of the neutrophil in rheumatoid arthritis. *Clin. Orthop.* **265**, 63–72 (1991).
- Kowanko, I.C., Ferrante, A., Clemente, G., Youssef, P.P. & Smith, M. Tumor necrosis factor priming of peripheral blood neutrophils from rheumatoid arthritis patients. *J. Clin. Immunol.* **16**, 216–221 (1996).
- Mohr, W., Pelster, B. & Wessinghage, D. Polymorphonuclear granulocytes in rheumatic tissue destruction. VI. The occurrence of PMNs in menisci of patients with rheumatoid arthritis. *Rheumatol. Int.* **5**, 39–44 (1984).
- Wipke, B.T. & Allen, P.M. Essential role of neutrophils in the initiation and progression of a murine model of rheumatoid arthritis. *J. Immunol.* **167**, 1601–1608 (2001).
- Nandakumar, K.S., Svensson, L. & Holmdahl, R. Collagen type II-specific monoclonal antibody-induced arthritis in mice: description of the disease and the influence of age, sex, and genes. *Am. J. Pathol.* **163**, 1827–1837 (2003).
- Johnson, Z. *et al.* Chemokine inhibition—why, when, where, which and how? *Biochem. Soc. Trans.* **32**, 366–377 (2004).
- Wetzker, R. & Rommel, C. Phosphoinositide 3-kinases as targets for therapeutic intervention. *Curr. Pharm. Des.* **10**, 1915–1922 (2004).
- Camps, M. *et al.* Use of a scintillating solid support coated with an aminoglycoside for identifying and/or quantifying a radiolabeled aminoglycoside binding molecule such as

- mono- or polyphosphated phosphoinositide in a sample. in *WO2002101084* (Applied Research Systems Ars Holding N.V., 2002).
31. Weiss-Haljiti, C. *et al.* Involvement of phosphoinositide 3-kinase gamma, Rac, and PAK signaling in chemokine-induced macrophage migration. *J. Biol. Chem.* **279**, 43273–43284 (2004).
  32. Lopez-Illasaca, M., Crespo, P., Pellici, P.G., Gutkind, J.S. & Wetzker, R. Linkage of G protein-coupled receptors to the MAPK signaling pathway through PI 3-kinase gamma. *Science* **275**, 394–397 (1997).
  33. Henderson, R.B., Hobbs, J.A., Mathies, M. & Hogg, N. Rapid recruitment of inflammatory monocytes is independent of neutrophil migration. *Blood* **102**, 328–335 (2003).
  34. Kerwar, S.S. *et al.* Type II collagen-induced arthritis. Studies with purified anticollagen immunoglobulin. *Arthritis Rheum.* **26**, 1120–1131 (1983).
  35. Katso, R. *et al.* Cellular function of phosphoinositide 3-kinases: implications for development, homeostasis, and cancer. *Annu. Rev. Cell Dev. Biol.* **17**, 615–675 (2001).
  36. Carpenter, C.L. & Cantley, L.C. Phosphoinositide kinases. *Curr. Opin. Cell Biol.* **8**, 153–158 (1996).
  37. Firestein, G.S. Evolving concepts of rheumatoid arthritis. *Nature* **423**, 356–361 (2003).
  38. Yoshino, S. & Cleland, L.G. Depletion of alpha/beta T cells by a monoclonal antibody against the alpha/beta T cell receptor suppresses established adjuvant arthritis, but not established collagen-induced arthritis in rats. *J. Exp. Med.* **175**, 907–915 (1992).
  39. Seki, N. *et al.* Type II collagen-induced murine arthritis. I. Induction and perpetuation of arthritis require synergy between humoral and cell-mediated immunity. *J. Immunol.* **140**, 1477–1484 (1988).
  40. Rueckle, T., Jiang, X., Gaillard, P., Church, D. & Vallotton, T. Azolidinone-vinyl fused-benzene derivatives. in *WO2004007491* (Applied Research Systems Ars Holding N.V., 2004).
  41. Collaborative Computational Project Number 4. *Acta Crystallogr. D Biol Crystallogr.* **D50**, 760–763 (1994).
  42. Walker, E.H. *et al.* Structural determinants of phosphoinositide 3-kinase inhibition by wortmannin, LY294002, quercetin, myricetin, and staurosporine. *Mol. Cell* **6**, 909–919 (2000).